IEEE Access
Multidisciplinary | Rapid Review | Open Access Journal

Received October 19, 2017, accepted December 13, 2017, date of publication December 27, 2017,
date of current version February 14, 2018.

Digital Object Identifier 10.1109/ACCESS.2017.2784834

Robust Optimal Operation of AC/DC Hybrid Microgrids Under Market Price Uncertainties

AKHTAR HUSSAIN, (Student Member, IEEE), VAN-HAI BUI, (Student Member, IEEE), AND HAK-MAN KIM, (Senior Member, IEEE)
Department of Electrical Engineering, Incheon National University, Incheon 22012, South Korea

Corresponding author: Hak-Man Kim (e-mail: hmkim@inu.ac.kr)

This work was supported by the Korea Institute of Energy Technology Evaluation and Planning and the Ministry of Trade, Industry & Energy of South Korea under Grant 20168530050030.

ABSTRACT Energy management system (EMS) is responsible for the optimal operation of microgrids. EMS adjusts its operational schedule for near future by using the available information. Market price signals are generally used for the operation of microgrids, which are obtained by using estimation/ forecasting methods. However, it is difficult to precisely predict the market prices due to the involvement of various complex factors like weather, policy, demand, errors in forecasting methods, and fuel cost. Therefore, in this paper, the uncertainties associated with the real-time market price signals (buying and selling) are realized via a robust optimization method. In addition to market price signals, uncertainties associated with renewable power sources and forecasted load values are also considered. Initially, a deterministic model is formulated for an ac/dc hybrid microgrid. Then a min–max robust counterpart is formulated by considering the worst-case uncertainties. Finally, an equivalent mixed integer problem is formulated by using linear duality and other optimality conditions. The developed model can provide feasible solutions for all the scenarios if the uncertainties fluctuate within the specified bounds. The effect of market price uncertainties on internal power transfer and external power trading, operation cost, the state-of-charge of energy storage elements, and unit commitment of dispatchable generators is analyzed. Taguchi's orthogonal array (OA) method is used to find the worst-case scenario within the specified uncertainty bounds. Then, Monte Carlo method is used to generate various scenarios within the uncertainty bounds to evaluate the robustness of the selected scenario via Taguchi's OA method. Finally, a violation index is formulated to evaluate the robustness of the proposed approach against the deterministic model. Simulations results have validated the robustness of the proposed optimization strategy.

INDEX TERMS Forecasted price uncertainty, ac/dc hybrid microgrids, microgrid operation, optimal operation, robust optimization, uncertainty modeling.

NOMENCLATURE

A. IDENTIFIERS AND BINARY VARIABLES

t	Index of time, running from 1 to T.
g	Index of dispatchable generators, running from 1 to G.
g_{ac}, g_{dc}	Identifiers for AC and DC side generators.
$s_{t,g}$	Commitment identifier of dispatchable generator g.
$su_{t,g}$	Start-up identifier of dispatchable generator g.
$sd_{t,g}$	Shutdown identifier of dispatchable generator g.
$c_{t,x}$, $d_{t,x}$	Charging/discharging identifiers for x-side MG.
c_t^{DC}, d_t^{DC}	Charging/discharging identifiers for EV.

B. VARIABLES AND CONSTANTS

$C(P_{t,g}^{CDG})$	Generation cost of dispatchable unit g (KRW/kWh).
$P_{t,g}^{CDG}$	Amount of power generated by generator g (kWh).
$SUC_{t,g}^{CDG}$	Start-up cost of dispatchable unit g (KRW).
$SDC_{t,g}^{CDG}$	Shutdown cost of dispatchable unit g (KRW).
C_t^{Buy}, C_t^{Sell}	Power trading price with utility grid (KRW/kWh).
P_t^{Buy}, P_t^{Sell}	Amount of power traded with utility grid (kWh).
$P_{t,x}^{Load}$	Forecasted electric load of x-side microgrid (kWh).

$P_{t,x}^{BEC}$, $P_{t,x}^{BED}$	Amount of electricity charged/discharged to/from BESS of x-side MG (kWh).
$P_{t,DC}^{EVC}$, $P_{t,DC}^{EVD}$	Amount of electrical energy charged/ discharged to/from EV (kWh).
P_t^{FAC}, P_t^{TAC}	Amount of power received from AC side MG and sent to AC side MG, respectively (kWh).
P_t^{FDC}, P_t^{TDC}	Amount of power received from DC side MG and sent to DC side MG, respectively (kWh).
$P_{t,x}^{RDG}$	Output power of x-side renewable units (kWh).
ILC^{cap}, η^{ILC}	Capacity [kWh] and efficiency [%] of ILC.
BE_x^{cap}, EV_x^{cap}	Capacity of BESS and EV in x-side MG [kWh].
SOC_x^{BE}	SOC of BEES in x side microgrid [%].
SOC_{DC}^{EV}	SOC of EV [%].
η_x^{BEC}, η_x^{BED}	Charging/discharging loss of x side BESS [%].
η_{DC}^{EVC}, η_{DC}^{EVD}	Charging/discharging loss of EV [%].
P_{Con}^{EV}, SOC_{Tar}^{EV}	EV's contribution [kWh] and target SOC [%].
${}_t^{Buy}$, d_t^{Buy}	Bounded buying price [KRW/kWh] and associated uncertainty bound [kWh].
${}_t^{Sell}$, d_t^{Sell}	Bounded selling price [KRW/kWh] and associated uncertainty bound [kWh].
${}_{t,x}^{Load}$, $P_{t,x}^{RDG}$	Bounded load and renewable power [kWh].
$\Delta P_{t,x}^{Load}$	Uncertainty bound for load [kWh].
$\Delta P_{t,x}^{RDG}$	Uncertainty bound for renewable power [kWh].
$\overline{P}_{t,x}^{Load}$, $\overline{P}_{t,x}^{RDG}$	Upper bound for load and renewable [kWh].
$\overline{d}_t^{Buy}$, $\overline{d}_t^{Sell}$	Upper bound for buying/selling price [KRW/kWh].
$\underline{P}_{t,x}^{Load}$, $\underline{P}_{t,x}^{RDG}$	Lower bound for load and renewable [kWh].
$\underline{d}_t^{Buy}$, $\underline{d}_t^{Sell}$	Lower bound for buying/selling price [KRW/kWh].
$\varsigma_{t,b}$, $\lambda_{t,b}$	Dual variables for buying price [KRW].
$\varsigma_{t,s}$, $\lambda_{t,s}$	Dual variables for selling price [KRW].
π_t^{Buy}, π_t^{Sell}	Dual variables for buying and selling price [KRW].
$\Gamma_{b,t}$, $\Gamma_{s,t}$	Budget of uncertainty for buying and selling price.
Γ_t, ς_t	Budget of uncertainty for load-renewable pair and dual variable [kWh].
$z_{t,x}^{Load}$, $\bar{z}_{t,x}^{Load}$	Scaled deviations for load.
$z_{t,x}^{RDG}$, $\bar{z}_{t,x}^{RDG}$	Scaled deviations for renewables.
$\lambda_{t,x}^{l-}$, $\lambda_{t,x}^{l+}$	Dual variables for load [kWh].
$\lambda_{t,x}^{r-}$, $\lambda_{t,x}^{r+}$	Dual variables for renewables [kWh].
v	Violation index for Monte Carlo scenarios [%].

I. INTRODUCTION

Microgrids have the potential to sustain the penetration of distributed energy sources and hence have the capability to enhance the service reliability and reduce the operation cost [1]. Microgrid operation faces new challenges due to intermittent nature of renewable energy sources, increasing demand, and weather-related events. A real-time market is considered as one of the potential solutions to these problems, which is beneficial for both network operators and the customers [2]. In such markets, the energy management system (EMS) of a microgrid adjusts its operational schedule for near future by using the available information. Generally, forecasted market price signals are used for the operation of microgrids, which are based on estimation/forecasting methods. Several forecasting techniques are available in the literature for forecasting of short time market prices [3]–[6].

In order to gain access to more recent data, instead of using natural gas prices and electricity load historical data, a regression model to forecast the evolution of natural gas prices, and a model based on artificial neural networks (ANN) to forecast electricity loads, are used by [3]. The results of these models are used as input for an electricity price forecast model. The authors in [4] have developed a method for forecasting the short time market price signals. The authors have used local informative vector machine along with kernel principal component analysis method to derive the forecasting method. In [5], two methods are proposed to predict the next-day electricity demand and daily price curves by using the information of past curves. The process is based on robust functional principal component analysis and nonparametric models. The economic effect of forecast errors is conducted by [6] and different industrial loads are examined.

As noted by [6], it is difficult to precisely predict the market prices due to the involvement of various complex factors like weather, policy, demand, and fuel cost. Therefore, consideration of price uncertainty in the operation of microgrids is challenging. Recently, various studies have been conducted for optimal operation and optimal bidding in the smart grids considering price uncertainties [7]–[12]. The decision making of generation companies under uncertain markets is analyzed by [7] and an information gap decision theory-based approach is developed. The developed scheme is capable of providing a comprehensive decision insight under risk-averse and risk-seeking behaviors. Optimal operation of demand response and energy storage systems for minimization of distribution losses are investigated in [8] under uncertain electricity prices. Participation of microgrids in pool markets

and operation of controllable loads with uncertain market prices are considered in [9]. The uncertainties are realized by using a two-stage stochastic method. A stochastic optimization approach is used by [10] for analyzing the impact of natural disasters on the operation of microgrids. In addition to market price uncertainties, uncertainties associated with renewable energy sources and electric vehicles are also considered by [10]. Effect of market price uncertainties on the bidding of microgrids is analyzed by [11] and [12]. A robust optimization approach is suggested by [11] for decision making of electricity retailers and optimal bidding strategy is also proposed considering the demand response programs. A hybrid stochastic/robust optimization approach is used by [12] for minimizing net cost for optimal bidding of microgrids considering uncertainties.

Various studies are available in the literature which have considered the uncertainties associated with renewable energy sources [13], [14], loads [15], [16], both renewables and loads [17], [18], and demand response programs [19], [20]. The uncertainty modeling techniques used by the researchers can be categorized as stochastic scenario-based modeling [21], robust optimization methods [22], and fuzzy modeling [23]. The merits and demerits of each modeling technique can be found in [17] and [18]. Due to the ability of the robust optimization method to provide a guaranteed immunity against worst-case realization and reduction in computational burden, it has gained popularity among the researchers. Therefore, various forms of robust optimization techniques are used by different researchers for optimal operation of microgrids with given uncertainty bounds [13], [17], [18].

Plenty of literature is available for operation of microgrids while considering uncertainties associated with renewable energy sources and/or forecasted loads, as mentioned in the previous paragraph. However, studies considering market price uncertainties are limited, as noted by [9]. The available studies considering uncertainty in market price signals are mostly concentrated on demand response programs and/or bidding strategies. Studies considering the effect of market price uncertainty on the operation of microgrids are limited. In addition, most of the studies have used stochastic optimization techniques for realization of uncertainties associated with market prices. The complexity of stochastic problems increases drastically with increase in the problem size and they can only provide a probabilistic guarantee against the feasibility of the solution. Therefore, mixed integer linear programming (MILP)-based optimization strategies are required, which can be easily implemented by using commercial optimization tools.

II. EXISTING LITERATURE AND CONTRIBUTIONS

As mentioned in the previous paragraphs, uncertainties in loads and/or renewables are focused in the existing literature. As noted by [9], studies considering market price uncertainties are limited. Studies related to the impact of market price uncertainties are also mainly focused on demand response programs and/or bidding strategies. Therefore, the effect of real-time market price uncertainties on the operation of AC/DC hybrid microgrids is analyzed in this paper. The effect of market price uncertainties on the operation of dispatchable generators, i.e. controllable distributed generators (CDGs), battery energy storage system (BESS) units, internal power transfer, and external power trading are analyzed.

In addition, most of the studies available in the literature regarding market price uncertainties are based on stochastic optimization techniques. In the case of robust optimization, instead of accurate distribution functions, deterministic uncertainty bounds are required. In addition, the final problem is tractable and can be implemented by using commercial optimization tools. Therefore, uncertainties associated with market price are realized by using robust optimization method in this study. The validity of the proposed method is evaluated by simulating three different cases. In the first case, nominal values for selling price along with uncertain buying price are considered. In the second case, nominal values for buying price along with uncertain selling price are considered. In the third case, uncertainty in both buying and selling prices is considered. Finally, the robustness of the proposed method is evaluated using Taguchi's orthogonal array (OA) method to find the worst-case scenario among various possible scenarios. Then, Monte Carlo method is used to generate various scenarios within the uncertainty bounds to evaluate the robustness of the selected scenario.

The major contributions of this study in comparison with the existing literature can be summarized as follows:

- In contrast to the existing literature, where uncertainties associated with forecasted load values and output power of renewables are focused, the uncertainties of market price signals (buying and selling prices) are considered for an AC/DC hybrid microgrid in this study.
- In the existing literature, the effect of market price uncertainties on demand response programs and/or bidding strategies is focused while in this study; the effect of market price uncertainties on the operation of CDGs, BESS units, internal power transfer between AC & DC sides, and external power trading with the utility grid are analyzed.
- In contrast to the existing literature, where stochastic optimization methods are used for realizing the uncertainties of market price signals, the robust optimization method is used to develop a mixed integer linear programming formulation. In the case of robust optimization, deterministic uncertainty bounds are required and it can be easily implemented by using the available commercial software.
- The robustness of the developed model is evaluated by selecting a worst-case scenario via Taguchi's OA method among various possible scenarios. Finally, a violation index is formulated to evaluate the robustness of the proposed approach against the deterministic model.

III. OPERATION OF AC/DC HYBRID MICROGRIDS UNDER UNCERTAIN MARKET PRICES

EMS is responsible for the optimal operation of the resources of a microgrid and it is also responsible for communication with these components. Initially, due to the dominance of conventional power system with AC form, AC microgrids were developed [24]. Therefore, integration of renewable distributed generators (RDGs) with the conventional AC systems was widely studied [25]. Recently, DC microgrids and distribution systems are also taken into consideration due to the widespread of DC sources and loads [26]. Therefore, AC and DC microgrids were integrated to form AC/DC hybrid microgrids in order to get benefit from both types of microgrids. Due to above-mentioned merits, a AC/DC hybrid microgrid is considered in this study.

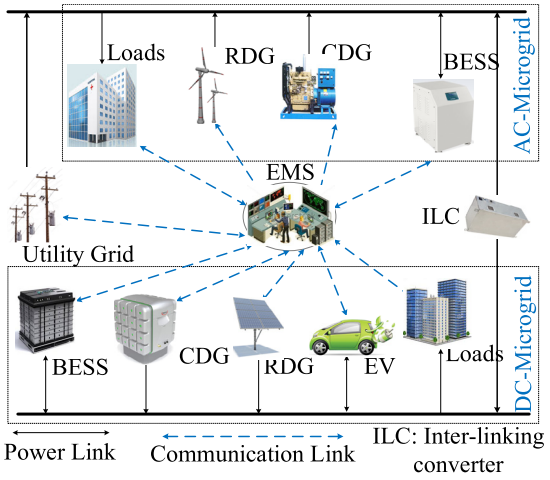

FIGURE 1. A typical AC/DC hybrid microgrid.

A. SYSTEM CONFIGURATION

A typical AC/DC hybrid microgrid, which is considered in this study also, is shown in Figure 1. The AC side microgrid contains CDGs, wind turbine, BESS, and AC loads. Similarly, the DC side microgrid contains photovoltaic cell, CDGs, BESS, electric vehicles (EVs), and DC loads. Utility grid is connected to the AC side microgrid and AC & DC microgrids are interlinked via an interlinking converter. Both AC and DC side microgrids have BESS units to increase their reliability even if there is any abnormal condition in the interlinking converter. The amount of power transferred between AC and DC side microgrids and power traded by DC microgrid will be constrained by the capacity of the interlinking converter.

EMS is primarily responsible for receiving information from all the components of both AC and DC microgrids and their operation. Market price signals are received from the utility grid for the operation of the microgrid. The operation horizon of EMS is taken as 24-hours (T) with a time step of 1 hour (t). The operation horizon for an EV (τ) is the time between its arrival (t_a) and departure (t_d).

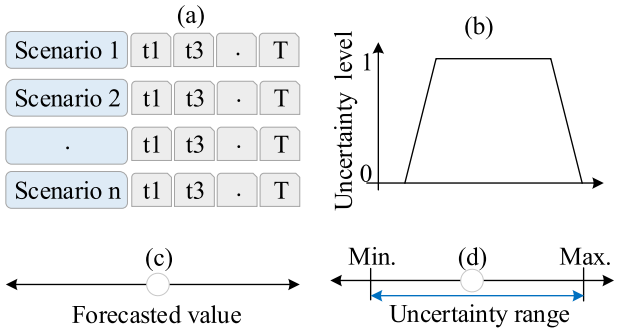

FIGURE 2. (a) Stochastic modeling; (b) Fuzzy formulation; (c) Deterministic modeling; (d) Robust optimization.

B. UNCERTAINTY MODELING

Several techniques are available in the literature for modeling uncertainties associated with microgrids. Broadly, these techniques can be divided into three major categories, i.e. stochastic scenario-based techniques (Figure 2a), fuzzy modeling techniques (Figure 2b), and robust optimization techniques (Figure 2d) [8]. In deterministic modeling techniques (Figure 2c), uncertainties are not considered and optimization is based on forecasted values. In stochastic optimization, probability density functions of the uncertain parameters are used and various scenarios are formulated. In the case of fuzzy modeling, membership functions of uncertain parameters are used to evaluate the degree of uncertainty. Finally, in the case of robust optimization, upper and lower bounds of uncertain parameters are used to provide a feasible solution for the worst-case scenario. The pros and cons of these techniques are summarized in [8] and [17] and it is concluded that robust optimization is superior to other uncertainty handling techniques.

C. PROPOSED METHOD

A modified robust optimization technique, as suggested by [27], is used in this paper to realize the uncertainties associated with market prices, loads, and renewables. The step-by-step process of the proposed uncertainty handling model is shown in Figure 3. The first step is to formulate a deterministic model. Considering the worst-case scenario, a robust counterpart is formulated in the second step. The robust counterpart is usually a min-max problem. Therefore, the inner max part is considered as a subproblem and its dual is formulated in the third step. Finally, a robust tractable problem is formulated using dual and the robust counterpart.

IV. PROBLEM FORMULATION

In this section, mathematical modeling of the proposed optimization scheme is presented, in accordance with Figure 3. The first step is to formulate a deterministic model, which is explained in the following section. The control of microgrids is divided into several levels due to the difference in time scale and significance of each control level [28]. Optimal operation of microgrids is considered as the uppermost level of microgrid control. Each lower level of control is a prerequisite for the upper-level control [17]. Therefore, constraints

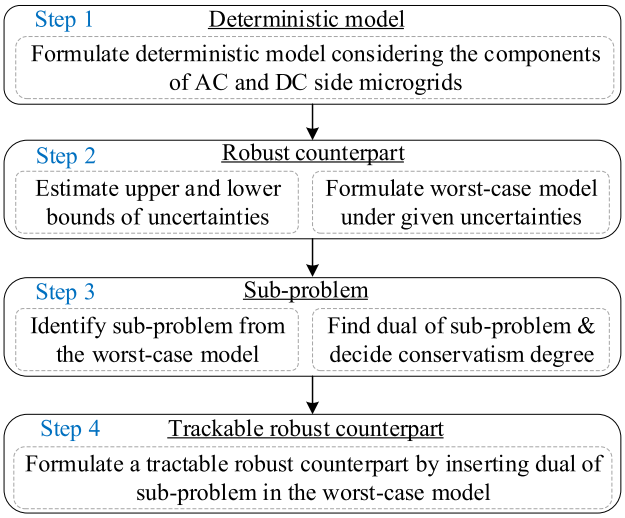

FIGURE 3. Uncertainty-modeling process in robust optimization.

related to the lower levels' control are assumed to be satisfied in each of the upper-level control. The proposed approach is meant for optimal operation of microgrids, therefore, lower level controls like internal voltage and current control of distributed generators, voltage and frequency deviations compensation, and current levels, have not been included(assumed to be fulfilled). The line losses in microgrids are negligible [29], therefore, lines losses are not considered. However, the loss of interlinking converter is incorporated in the optimization model.

A. DETERMINISTIC MODEL

1) OBJECTIVE FUNCTION

The cost function of the hybrid microgrid is the total expenses occurred for the hybrid microgrid when external trading of electricity is applied as given by (1). The first term of the objective function contains the generation cost ($C^{CDG}_{g_{ac}}(P^{CDG}_{t,g_{ac}})$), start-up cost ($SUC^{CDG}_{t,g_{ac}}$), and shut down cost ($SDC^{CDG}_{t,g_{ac}}$) of AC side CDGs. The second term contains the generation cost ($C^{CDG}_{g_{dc}}(P^{CDG}_{t,g_{dc}})$), start-up cost ($SUC^{CDG}_{t,g_{dc}}$), and shut down cost ($SDC^{CDG}_{t,g_{dc}}$) of DC side CDGs. The third and fourth terms contain the profit gained by trading power with the utility grid ($C^{Buy}_t.P^{Buy}_t - C^{Sell}_t.P^{Sell}_t$). The total amount of power trading between the hybrid microgrid and the utility grid can be obtained by summing the power traded by individual AC and DC side microgrids. The amount of power traded with the utility grid by the DC microgrid is

$$\begin{aligned} &C^{MG}\left(P^{CDG}_{t,g_{ac}}, P^{CDG}_{t,g_{dc}}, P^{Buy}_t, P^{Sell}_t, s_{t,g_{ac}}, s_{t,g_{dc}}\right) \\ &= \sum_{t\in T}\sum_{g_{ac}\in G_{ac}}\left(C^{CDG}_{g_{ac}}(P^{CDG}_{t,g_{ac}}) + SUC^{CDG}_{t,g_{ac}} + SDC^{CDG}_{t,g_{ac}}\right) \\ &\quad + \sum_{t\in T}\sum_{g_{dc}\in G_{dc}}\left(C^{CDG}_{g_{dc}}(P^{CDG}_{t,g_{dc}}) + SUC^{CDG}_{t,g_{dc}} + SDC^{CDG}_{t,g_{dc}}\right) \\ &\quad + \sum_{t\in T} C^{Buy}_t.P^{Buy}_t - \sum_{t\in T} C^{Sell}_t.P^{Sell}_t \end{aligned} \tag{1}$$

where,

$$P^{Buy}_t = P^{Buy}_{t,AC} + \frac{P^{Buy}_{t,DC}}{\eta^{ILC}}, \quad P^{Sell}_t = P^{Sell}_{t,AC} + \eta^{ILC}.P^{Sell}_{t,DC}$$

constrained by the efficiency of the interlinking converter (η^{ILC}). $s_{t,g_{ac}}$ and $s_{t,g_{dc}}$ indicate the commitment status of AC and DC side CDGs, respectively. The commitment status of CDGs is used to compute the startup and shutdown costs. Let $P^{MG}_t = \left\{P^{CDG}_{t,g_{ac}}, P^{CDG}_{t,g_{dc}}, P^{Buy}_t, P^{Sell}_t, s_{t,g_{ac}}, s_{t,g_{dc}}\right\}$ be the set of control variables for deciding the operation cost of the hybrid microgrid by the deterministic model. Then, the objective of the deterministic model is to minimize the overall cost of the hybrid microgrid as follows:

$$P^{MG^*} = \arg\min\left\{C^{MG}(P^{MG^*}_t)\right\}$$

2) LOAD BALANCING CONSTRAINTS

The AC side load should be balanced with the amount of power generated by the AC side RDG, CDGs, power charged/discharged to/from BESS, power transferred between AC and DC side microgrids, and power traded with the utility grid, as given by (2). Similarly, energy balancing of DC side microgrid is given by equation (3). Power can be sent from the AC side microgrid to the DC side microgrid and vice versa in order to reduce the operation cost of the network by sharing more economical components. This sharing of power between the AC and the DC side microgrids is termed as internal power transfer in this paper. The internal power transfer can be modeled by using Equation (4). Interlinking converter loss is considered for internal power transfer between AC and DC side microgrids as given by (4). The amount of power traded between DC side microgrid and the utility grid is constrained by the capacity of the interlinking converter as given by (5). It is the same case for power transfer between AC and DC side microgrids, as depicted by (5).

$$P^{RDG}_{t,AC} + \sum_{g_{ac}\in G_{ac}} P^{CDG}_{t,g_{ac}} + P^{BEC}_{t,AC} - P^{BED}_{t,AC} + P^{Tr}_{t,AC} = P^{Load}_{t,AC} \tag{2}$$

Where,

$$\begin{aligned} P^{Tr}_{t,AC} &= \eta^{ILC}.P^{FDC}_t - P^{TDC}_t + P^{Buy}_{t,AC} - P^{Sell}_{t,AC} \\ P^{RDG}_{t,DC} &+ \sum_{g_{dc}\in G_{dc}} P^{CDG}_{t,g_{dc}} + P^{BEC}_{t,DC} - P^{BED}_{t,DC} + P^{EVC}_{t,DC} \\ &- P^{EVD}_{t,DC} + P^{Tr}_{t,DC} = P^{Load}_{t,DC} \end{aligned} \tag{3}$$

Where,

$$P^{Tr}_{t,DC} = \eta^{ILC}.P^{FAC}_t - P^{TAC}_t + \frac{P^{Buy}_{t,DC}}{\eta^{ILC}} - \eta^{ILC}.P^{Sell}_{t,DC}$$

$$P^{FDC}_t = \eta^{ILC}.P^{TAC}_t, P^{FAC}_t = \eta^{ILC}.P^{TDC}_t \tag{4}$$

$$P^{TDC}_t + P^{Buy}_{t,DC} \le ILC^{cap}, P^{TAC}_t + P^{Sell}_{t,DC} \le ILC^{cap} \tag{5}$$

3) CONTROLLABLE GENERATOR CONSTRAINTS

The generation bounds for gth CDG unit are given by (6), where g indicates the total number of CDGs in the hybrid microgrid, i.e. $g = g_{ac} + g_{dc}$. The binary variable $s_{t,g}$ shows the commitment status of CDG g at t. The value of this binary variable is 1, if CDG is committed to operate at time t, and 0 otherwise. The unit commitment status can be used to determine the start-up and shut down time of g^{th} CDG by using (7). Equation (7) shows the relation between the shutdown indicator ($sd_{t,g}$) and start-up indicator ($su_{t,g}$). Equations (8) and (9) show the constraints for start-up and shut down costs, respectively. Equation (10) shows that CDGs cannot be started up and shut down simultaneously.

$$\min[P_g^{CDG}].s_{t,g} \le P_{t,g}^{CDG} \le \max[P_g^{CDG}].s_{t,g};\ s_{t,g} \in \{0,1\} \tag{6}$$

$$su_{t,g} - sd_{t,g} = s_{t,g} - s_{t-1,g} \tag{7}$$

$$SUC_{t,g}^{CDG} \ge UC_{t,g}^{CDG}.\left(s_{t,g} - s_{t-1,g}\right);\quad SUC_{t,g}^{CDG} \ge 0 \tag{8}$$

$$SDC_{t,g}^{CDG} \ge DC_{t,g}^{CDG}.\left(s_{t-1,g} - s_{t,g}\right);\quad SDC_{t,g}^{CDG} \ge 0 \tag{9}$$

$$su_{t,g} + sd_{t,g} \le 1;\quad su_{t,g}, sd_{t,g} \in \{0,1\} \tag{10}$$

4) BATTERY CONSTRAINTS

The constraints for power stored in the BESS of x side microgrid are given by Equations (11) and (12), where "x" will be replaced with AC or DC for AC and DC side BESS. Equations (13) and (14) show the charging and discharging limits of x side BESS, respectively. Equation (15) shows the constraints for initial and final steps of the simulation period with SOC_x^{INIT} as the initial SOC of x side BESS unit. Equation (16) shows that simultaneous charging and discharging of BESS is not allowed.

$$\min[BE_x^{cap}] \le SOC_x^{BE} \le \max[BE_x^{cap}] \tag{11}$$

$$SOC_{t,x}^{BE} = SOC_{t-1,x}^{BE} + P_{t,x}^{BEC}.\eta_x^{BEC} - \frac{P_{t,x}^{BED}}{\eta_x^{BED}} \tag{12}$$

$$0 \le P_{t,x}^{BEC} \le \frac{\left(\max[BE_x^{cap} - SOC_{t-1,x}^{BE}]\right)}{\eta_x^{BEC}}.\mathrm{c}_{t,x} \tag{13}$$

$$0 \le P_{t,x}^{BED} \le \eta_x^{BED}.\left(SOC_{t-1,x}^{BE} - \min[BE_t^{cap}]\right).\mathrm{d}_{t,x} \tag{14}$$

$$SOC_{t,x}^{BE} \le 0 \quad if\ \mathrm{t} = \mathrm{T};\quad SOC_{t-1,x}^{BE} = SOC_x^{INIT}\ if\ \mathrm{t} = 1 \tag{15}$$

$$\mathrm{c}_{t,x} + d_{t,x} = 1;\quad \mathrm{c}_{t,x}, d_{t,x} \in \{0,1\};\quad 0 \le \eta_x^{BED}, \eta_x^{BEC} \le 1 \tag{16}$$

5) ELECTRIC VEHICLE CONSTRAINTS

The constraints related to the charging, discharging, and SOC computation of EVs are similar to those of BESS units, as given by equations (17)-(20). However, EVs can only be used between their time of arrival to time of departure, as given by (21). The contribution of an EV during its period of stay can be computed by using (23), where $m = 1$ indicates the vehicle-to-grid mode, $m = -1$ indicates grid-to-vehicle mode, and $m = 0$ indicates the idle mode. The SOC of EV needs to be above the target level before its departure time, as depicted by equation (22). Similar to BESS, EVs can also be in one of their operation modes (charging or discharging) at a given time interval, as given by (24).

$$\min[EV_{DC}^{cap}] \le SOC_{DC}^{EV} \le \max[EV_{DC}^{cap}] \tag{17}$$

$$SOC_{t,DC}^{EV} = SOC_{t-1,DC}^{EV} + P_{t,DC}^{EVC}.\eta_{DC}^{EVD} - \frac{P_{t,DC}^{EVD}}{\eta_{DC}^{EVD}} \tag{18}$$

$$0 \le P_{t,DC}^{EVC} \le \frac{\left(\max[EV_{DC}^{cap} - SOC_{t-1,DC}^{EV}]\right)}{\eta_{DC}^{EVC}}.\mathrm{c}_t^{DC};\quad \mathrm{c}_t^{DC} + d_t^{DC} = 1 \tag{19}$$

$$0 \le P_{t,DC}^{EVD} \le \eta_{DC}^{EVD} \cdot \left(SOC_{t-1,DC}^{EV} - \min[EV_t^{cap}]\right).\mathrm{d}_t^{DC} \tag{20}$$

$$SOC_{t,DC}^{EV} = P_{t,DC}^{EVC} = P_{t,DC}^{EVD} = 0 \tag{21}$$

$$SOC_{t_d,DC}^{EV} = SOC_{t_a,DC}^{EV} + P_{Con}^{EV} \ge SOC_{Tar}^{EV} \tag{22}$$

$$P_{Con}^{EV} = \sum_{t\in[t_a,t_d]} \left(P_{t,DC}^{EVD} - P_{t,DC}^{EVC}\right).m_t;\quad m_t \in \{-1,0,1\} \tag{23}$$

$$\mathrm{c}_t^{DC} + d_t^{DC} = 1, \mathrm{c}_t^{DC}, d_t^{DC} \in \{0,1\};\quad 0 \le \eta_{DC}^{EVD}, \eta_{DC}^{EVC} \le 1 \tag{24}$$

B. ROBUST COUNTERPART: MARKET PRICE

The uncertain parts in the objective function are buying price (C_t^{Buy}) and selling price (C_t^{Sell}). The uncertainty associated with the buying part and the selling part can be treated as two separate problems. The inner max problems inside the objective function are identified and are treated as sub-problems. Dual of these sub-problems is obtained to transform the min-max problem into a tractable problem.

1) PRICE UNCERTAINTY MODELING

The objective function of the robust model needs to consider the uncertainties associated with buying and selling price signals. The electric power balance in the microgrid should be met when the worst-case of uncertainties occur. The uncertainty associated with each entry of buying price C_t^{Buy}, t ∈ T takes values in $[\mathrm{C}_t^{Buy} + d_t^{Buy}]$, where d_t^{Buy} is the deviation from the nominal price coefficient C_t^{Buy} [27]. The uncertain buying price signal ($_t^{Buy}$) at each time interval along with the bounds of deviations is given by (25). Similarly, the uncertainty associated with each entry of selling price C_t^{Sell}, t ∈ T takes values in $[\mathrm{C}_t^{Sell} + d_t^{Sell}]$, where d_t^{Sell} is the deviation from the nominal price coefficient C_t^{Sell}. The uncertain selling price signal ($_t^{Sell}$) at each time interval along with the bounds of deviations is given by (26). The constraints for upper and lower bounds are given by (27), which can be computed by using methods suggested by [30], [31]. The upper and lower bounds can be obtained by taking a specified percentage of

the nominal price values [11], [12], [18], i.e. ±20% of the nominal values.

$$\overleftrightarrow{C}_t^{Sell} = C_t^{Sell} + d_t^{Sell} \tag{25}$$

where,

$$\begin{aligned} \underline{d}_t^{Sell} - C_t^{Sell} \le d_t^{Sell} \le \overline{d}_t^{Sell} - C_t^{Sell} \\ \overleftrightarrow{C}_t^{Buy} = C_t^{Buy} + d_t^{Buy} \\ \underline{d}_t^{Buy} - C_t^{Buy} \le d_t^{Buy} \le \overline{d}_t^{Buy} - C_t^{Buy} \end{aligned} \tag{26}$$

$$\underline{d}_t^{Buy}, \underline{d}_t^{Sell}, \overline{d}_t^{Buy}, \overline{d}_t^{Sell} \ge 0; \quad d_t^{Sell}, d_t^{Buy} \; free \tag{27}$$

2) ROBUST COUNTERPART

The robust counterparts of both buying part and selling part can be computed by using the method suggested by [27]. The robust counterpart of buying part is given by Equations (28), (29). Similarly, the robust counterpart of selling part is given by (30), (31). Both of the robust counterparts are min-max problems, therefore, the inner sub-problems will be transformed to linearize the problems. Γ_b is the budget of uncertainty parameter for buying price and Γ_s is the budget of uncertainty parameter for selling price. The budget of uncertainty can be used to control the conservatism of the solution and to adjust the probability of infeasible solution.

$$\min\left\{\mathbf{C}^{Buy}, \mathbf{P}^{Buy}\right\} + \max_{\{S_o|S_o\subseteq T_o, |S_o|\le\Gamma_b\}} \sum_{t\in S_o} d_t^{Buy}|P_t^{Buy} \tag{28}$$

$$\text{Subject to} P_{\min}^{Buy} \le \mathbf{P}^{Buy} \le P_{\max}^{Buy}; \quad \text{Equations (2)-(5)} \tag{29}$$

$$\min\left\{\mathbf{C}^{Sell}, \mathbf{P}^{Sell}\right\} + \max_{\{S_o|S_o\subseteq T_o, |S_o|\le\Gamma s\}} \sum_{t\in S_o} d_t^{Sell}|P_t^{sell} \tag{30}$$

$$\text{Subject to } P_{\min}^{Sell} \le \mathbf{P}^{Sell} \le P_{\max}^{Sell}; \quad \text{Equations (2)-(5)} \tag{31}$$

3) SUB-PROBLEM AND TRANSFORMATION

The inner maximization problem of buying part is taken as the objective function with (29) and (2)-(5) as the constraints.

This type of problems have an equivalent mixed integer problem (MIP) formulation as given by Equations (32)-(35). The proof of this transformation can be found in [27]. In these equations, $\varsigma_{t,b}$, $\lambda_{t,b}$, π_t^{Buy} are the dual variables, which are introduced for transforming the inner sub-problem of buying part into its dual.

$$\min\left\{\mathbf{C}^{Buy}.\mathbf{P}^{Buy} + \varsigma_{t,b}.\Gamma_{t,b} + \sum\lambda_{t,b}\right\} \tag{32}$$

$$\text{Subject to } \varsigma_{t,b} + \lambda_{t,b} \ge d_t^{Buy}.\pi_t^{Buy} \tag{33}$$

$$\pi_t^{Buy} \ge 0; \quad \varsigma_{t,b} \ge 0 \tag{34}$$

$$-\pi_t^{Buy} \le P_t^{Buy} \le \pi_t^{Buy} \tag{35}$$

Similarly, the robust counterpart of selling part can also be transformed into its equivalent MIP form as given by Equations (36)-(39). These two transformed subproblems can be inserted back to the original deterministic objective function to form a tractable robust counterpart. In Equations (36)-(39), $\varsigma_{t,s}$, $\lambda_{t,s}$, π_t^{Sell} are the dual variables for transforming the inner sub-problem into its dual.

$$\min\left\{\mathbf{C}^{Sell}.\mathbf{P}^{Sell} + \varsigma_{t,s}.\Gamma_{t,s} + \sum\lambda_{t,s}\right\} \tag{36}$$

$$\text{Subject to } \varsigma_{t,s} + \lambda_{t,s} \ge -d_t^{Sell}.\pi_t^{Sell} \tag{37}$$

$$\pi_t^{Sell} \ge 0; \quad \varsigma_{t,s} \ge 0 \tag{38}$$

$$-\pi_t^{Sell} \le P_t^{Sell} \le \pi_t^{Sell} \tag{39}$$

C. ROBUST COUNTERPART: RENEWABLES & LOAD

The load balancing equations of the deterministic model, (2), (3), contain uncertain factor like output power of renewables and forecasted load values. The uncertainty in load can be modeled as (40), (41), where "x" represents the AC or DC side of the microgrid. Similarly, the uncertainty in the renewables can be modeled as (42), (43).

$$\overleftrightarrow{P}_t^{Load} = P_{t,x}^{Load} + \Delta P_{t,x}^{Load} \tag{40}$$

$$\underline{P}_{t,x}^{Load} - P_{t,x}^{Load} \le \Delta P_{t,x}^{Load} \le \overline{P}_{t,x}^{Load} - P_{t,x}^{Load} \tag{41}$$

$$\overleftrightarrow{P}_t^{RDG} = P_{t,x}^{RDG} + \Delta P_{t,x}^{RDG} \tag{42}$$

$$\underline{P}_{t,x}^{RDG} - P_{t,x}^{RDG} \le \Delta P_{t,x}^{RDG} \le \overline{P}_{t,x}^{RDG} - P_{t,x}^{RDG} \tag{43}$$

1) SUB-PROBLEM

The worst-case of uncertainty in the load balancing will occur when the load takes the upper uncertainty bounds and renewables take the lower uncertainty bounds. Therefore, the following equation will be added to the load balancing equation to cater the worst-case uncertainties.

$$\max\left(\begin{pmatrix}\underline{z}_{t,x}^{Load}.\underline{P}_{t,x}^{Load} + \overline{z}_{t,x}^{Load}.\overline{P}_{t,x}^{Load}\end{pmatrix} - \begin{pmatrix}\underline{z}_{t,x}^{RDG}.\underline{P}_{t,x}^{RDG} + \overline{z}_{t,x}^{RDG}.\overline{P}_{t,x}^{RDG}\end{pmatrix}\right) \tag{44}$$

$$\text{Subject to } \underline{P}_{t,x}^{Load} + \overline{P}_{t,x}^{Load} + \underline{P}_{t,x}^{RDG} + \overline{P}_{t,x}^{RDG} \le \Gamma_t \tag{45}$$

$$0 \le \underline{z}_{t,x}^{Load}, \overline{z}_{t,x}^{Load}, \underline{z}_{t,x}^{RDG}, \overline{z}_{t,x}^{RDG} \le 1 \tag{46}$$

Γ_t is the budget of uncertainty for the load-renewable pair. It can be observed that Equation (44) is a new maximization problem inside the cost minimization function. Therefore, Equations (44)-(46) are considered as a sub-problem.

2) DUAL OF SUB-PROBLEM

Due to the presence of maximization sub-problem inside the cost minimization function, the problem becomes a min-max problem. Therefore, the dual of sub-problem (Equations (44)-(46)) is computed as follows [17].

$$\min\left\{\varsigma_t.\Gamma_t + \lambda_{t,x}^{l+} + \lambda_{t,x}^{l-} + \lambda_{t,x}^{r+} + \lambda_{t,x}^{r-}\right\} \tag{47}$$

$$\text{Subject to } \varsigma_t + \lambda_{t,x}^{l+} \ge \overline{P}_{t,x}^{Load}; \quad \varsigma_t + \lambda_{t,x}^{l-} \ge \underline{P}_{t,x}^{Load} \tag{48}$$

$$\varsigma_t + \lambda_{t,x}^{r+} \ge \overline{P}_{t,x}^{RDG}; \quad \varsigma_t + \lambda_{t,x}^{r-} \ge \underline{P}_{t,x}^{RDG} \tag{49}$$

$$\varsigma_t, \lambda_{t,x}^{l+}, \lambda_{t,x}^{l-}, \lambda_{t,x}^{r+}, \lambda_{t,x}^{r-} \ge 0 \tag{50}$$

In the sub-dual, Equation (47) is the objective function of the dual problem and Equations (48)-(50) are the constraints. ς_t, $\lambda_{t,x}^{l+}$, $\lambda_{t,x}^{l-}$, $\lambda_{t,x}^{r+}$, $\lambda_{t,x}^{r-}$ are the dual variables used for transforming the sub-problem into its dual.

D. BUDGET OF UNCERTAINTY

In both of the transformed problems, a new variable named as the budget of uncertainty (Γ_b, Γ_s, Γ) is added. This variable is used to control the conservatism of the solution. The relationship between the probability of a feasible solution and budget of uncertainty is given by (51) [22], where $\Phi(\theta)$ is the cumulative distribution function (CDF) of a standard normal distribution function. However, this function is only valid when $\Gamma_i = \theta\sqrt{n}$. Therefore, a more general approximate function is derived by [22], which is applicable for all cases, as given by Equation (52). The conservatism of the solution and the probability of an infeasible solution under the given uncertainty bounds can be controlled by selecting a suitable value of the budget of uncertainty. Equations (51) and (52) show the relationship between the probability of an infeasible solution ($B(n, \Gamma_i)$) and the budget of uncertainty (Γ_i). By varying the values of Γ_i, the probability of infeasible solutions can be evaluated.

$$\lim_{n\to\infty} B(n, \Gamma_i) = 1 - \Phi(\theta) \tag{51}$$

Where,

$$\Phi(\theta) = \frac{1}{\sqrt{2\pi}} \int_{-\infty}^{\theta} \exp\left(-\frac{y^2}{2}\right) dy$$
$$B(n, \Gamma_i) \approx 1 - \Phi(\frac{\Gamma_i - 1}{\sqrt{n}}) \tag{52}$$

The budget of uncertainty has the following properties.

- It can take any value between 0 and T, where T is the total number of time intervals.
- $\Gamma_i = 0$ indicates the nominal case (no uncertainty) and $\Gamma_i = T$ is the worst-case realization (uncertainty in all t).
- The higher the value of Γ_i the lesser is the probability of the infeasible solution and vice versa.

For a single time interval t, $\Gamma_{t,i}$ can take values between 0 and 1, i.e. $\Gamma_{t,i} \in [0, 1]$, where $\Gamma_{t,i} = 0$ indicates that uncertainty is not considered for that time interval (forecasted value). $\Gamma_{t,i} = 1$ indicates that uncertainty has taken its worst value at the given time interval t. Therefore, a tradeoff needs to be made by the decision makers by selecting an appropriate value of Γ_i for a given system.

E. TRACTABLE ROBUST COUNTERPART

Finally, a robust tractable counterpart is obtained by replacing the uncertain terms in the objective function by their transformed robust counterparts as given by Equation (53). It can be observed from equation (53) that, in addition to the control variables of the deterministic model ($P_{t,g}^{CDG}, P_t^{Buy}, P_t^{Sell}, s_{t,g}$), it also contains dual control variables ($\varsigma_{t,b}, \Gamma_{t,b}, \varsigma_{t,s}, \Gamma_{t,s}, \lambda_{t,b}, \lambda_{t,s}$). These dual variables are used to cater the uncertainties associated with market buying and selling prices.

$$\begin{aligned} C^{RMG}&\left(P_{t,g}^{CDG}, P_t^{Buy}, P_t^{Sell}, s_{t,g}, \varsigma_{t,b}, \Gamma_{t,b}, \varsigma_{t,s}, \Gamma_{t,s}, \lambda_{t,b}, \lambda_{t,s}\right) \\ &= \sum_{t\in T} \sum_{g_{ac}\in G_{ac}} \left(C_{g_{ac}}^{CDG}(P_{t,g_{ac}}^{CDG}) + SUC_{t,g_{ac}}^{CDG} + SDC_{t,g_{ac}}^{CDG}\right) \\ &\quad + \sum_{t\in T} \sum_{g_{dc}\in G_{dc}} \left(C_{g_{dc}}^{CDG}(P_{t,g_{dc}}^{CDG}) + SUC_{t,g_{dc}}^{CDG} + SDC_{t,g_{dc}}^{CDG}\right) \\ &\quad + \sum_{t\in T} \left(C_t^{Buy}.P_t^{Buy} + \varsigma_{t,b}.\Gamma_{t,b} + \sum \lambda_{t,b}\right) \\ &\quad - \sum_{t\in T} \left(C_t^{Sell}.P_t^{Sell} - \varsigma_{t,s}.\Gamma_{t,s} - \sum \lambda_{t,s}\right) \end{aligned} \tag{53}$$

Let

$$P_t^{RMG} = \{P_{t,g}^{CDG}, P_t^{Buy}, P_t^{Sell}, s_{t,g}, \varsigma_{t,b}, \Gamma_{t,b}, \varsigma_{t,s}, \Gamma_{t,s}, \lambda_{t,b}, \lambda_{t,s}\}$$

be the set of control variables for deciding the operation cost of the hybrid microgrid by the robust model. The objective of the robust model is to minimize the overall cost of the hybrid microgrid as follows:

$$P_t^{RMG*} = \arg\min \left\{C^{RMG}(P_t^{RMG})\right\}$$

Similarly, the trackable robust counterpart of load balancing equations can be obtained as follows.

$$\begin{aligned} P_{t,x}^{RDG} + \sum_{g_x\in G_x} P_{t,g_x}^{CDG} + P_{t,x}^{BE} + P_{t,x}^{Tr} + P_{t,DC}^{EV} \\ = P_{t,x}^{Load} + \varsigma_t.\Gamma_t + \lambda_{t,x}^{l+} + \lambda_{t,x}^{l-} + \lambda_{t,x}^{r+} + \lambda_{t,x}^{r-} \end{aligned}$$

Where,

$$P_{t,x}^{BE} = P_{t,x}^{BEC} - P_{t,x}^{BED}, P_{t,DC}^{EV} = P_{t,DC}^{EVC} - P_{t,DC}^{EVD} \tag{54}$$

The final trackable roust counterpart objective function is constrained by the following constraints.

Equations (2)-(27), (33)-(35), (37)-(43), (48)-(50), and (54).

F. ROBUSTNESS EVALUATION METHOD

The objective of this formulation is to make the system adapt to various market price scenarios and less sensitive to random deviations within the uncertainty bounds. If every variable of buying and selling price were represented by the selected levels, there would be many scenarios. It is computationally expensive to test all the scenarios, especially for large systems [18]. Therefore, the Taguchi's orthogonal array (OA) testing method is introduced in the robust design theory to select scenarios related to the uncertain variables [32]. Various methods for obtaining Taguchi's OAs can be found in [33] or can be obtained from [34]. A simple OA is shown in (55), where the first entity (4) shows the number of scenarios, the second entity (3) shows the number of variables, the third entity (2) shows the levels of each variable, and the

fourth entity (2) shows the strength of the OA.

$$OA(4,3,2,2) = \begin{bmatrix} 0 & 0 & 0 \\ 0 & 1 & 1 \\ 1 & 0 & 1 \\ 1 & 1 & 0 \end{bmatrix} \tag{55}$$

The number of testing scenarios is drastically reduced by Taguchi method, i.e. 2^3 scenarios are reduced to 4 in (55) for each cycle. Based on the levels of the variables different cycles could be produced by defining different rules. According to convex theory [35] and extreme solution theory [36], the extreme solutions exist in the endpoints of a linear problem. Therefore, Taguchi method can be applied to robust optimization by considering upper and lower bounds. In this study also, a small number of scenarios have been selected based on OA and corresponding rules. Finally, the worst-case scenario is selected and is analyzed for the variations of market price uncertainty.

By using the Taguchi method, the worst-case or most probable worst-case scenario can be determined but all scenarios cannot be tested. Therefore, Monte Carlo simulations are used to check the robustness of the selected scenario. Similar to [18], the robustness of the worst-case scenario is evaluated by defining a violation index as given by (56), where N is the total number of Monte Carlo simulations and N* is the number of scenarios violating the worst-case. A scenario violates the worst-case if the operation cost of the given scenario is greater than that of the worst-case scenario selected from OA. The worst-case for buying price occurs when it is close to the upper bound and that of selling price occurs when it is close to the lower bound. Therefore, the feasible region for Monte Carlo scenarios of buying price is between the forecasted values and the upper bounds. Similarly, the feasible region for selling price is between the forecasted values and the lower bounds. Finally, the feasibility of the robust management can be acceptable if v is within the acceptable range, i.e. $v \leq v^*$, where, v^* is a predefined acceptable criterion.

$$v = \frac{N*}{N}100 \tag{56}$$

V. NUMERICAL SIMULATIONS

The developed optimization scheme is applied to a AC/DC hybrid microgrid, as shown in Figure 1. Generally, the operation of microgrids is carried out for one day [6], [8]–[12], therefore, optimization in this study is also carried out for an operation horizon of 24-h with a 1 hour time interval. However, the time interval could be any uniform interval. CPLEX 12.3 is used as an optimization tool by integrating it with Java. The AC side microgrid contains two CDG units, a BESS unit, a wind turbine, and AC loads. The DC side microgrid contains two CDGs, a BESS unit, EVs, photovoltaic array, and DC loads. The voltage level of AC side microgrid is taken as 0.3kV and that of DC side microgrid as 0.7kV. The capacity of the interlinking converter is considered as 200kW with an efficiency of 97%.

TABLE 1. CDG parameters of the test system.

MGs	CDG1			CDG2		
	$P^{CDG}_{1,min}$ (kW)	$P^{CDG}_{1,max}$ (kW)	C^{CDG}_{1} (₩[1]/kWh)	$P^{CDG}_{2,min}$ (kW)	$P^{CDG}_{2,max}$ (kW)	C^{CDG}_{2} (₩[1]/kWh)
AC	0	100	100	0	120	116
DC	0	65	106	0	70	103
Total	0	165	-	0	190	-

[1]₩ is Korean Won (KRW)

TABLE 2. BESS and EV parameters of the test system.

MGs	η^{BEC}_{x} (%)	η^{BED}_{x} (%)	BE^{cap}_{x} (kWh)	η^{EVC}_{DC} (%)	η^{EVD}_{DC} (%)	EV^{cap}_{DC} (kWh)
AC	98	98	150	-	-	-
DC	98	98	150	98	98	100
Total	-	-	300	-	-	100

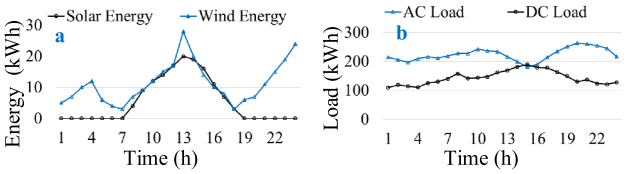

FIGURE 4. (a) Hourly renewable generation outputs; (b) Hourly electric load of AC and DC microgrids.

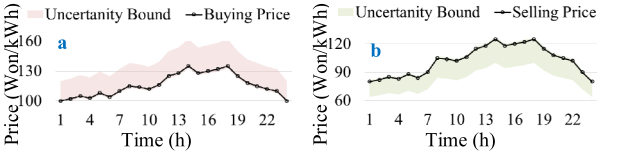

FIGURE 5. Hourly feasible uncertainty bounds: (a) Buying price; (b) Selling price.

A. INPUT DATA

The parameters related to CDGs are listed in Table 1 while the parameters of energy storage systems are tabulated in Table 2. The hourly output powers of renewable generators are shown in Figure 4a and hourly load profiles of both AC and DC microgrids are shown in Figure 4b. Figure 4 shows the worst-case scenario values, nominal values can be obtained by using the defined uncertainty bounds. The uncertainty bounds of buying prices are shown in Figure 5a and those of selling price are shown in Figure 5b. Where, buying price is the price, which will be paid by the microgrid owner while buying power from the utility grid. Contrarily, the price, which will be paid by the utility grid for buying power from the microgrid is termed as selling price. Generally, the buying and selling prices are different for microgrids [10], [11], [23]. The uncertainty bound for load is taken as ±10% for both AC and DC side microgrids. The uncertainty bound for renewables is taken as ±25% for both AC and DC side renewables. The uncertainty bounds of market signals are taken as ±20% of the nominal values in each time interval.

Theoretically, the market price signals can take any value from −20% to +20% of the nominal values. However, the

objective of the robust optimization is to provide immunity against the worst-case realization. The worst-case occurs when the buying price takes its upper bound and selling price takes its lower bound. Therefore, buying price bound will never take a negative value and selling price bound will never take a positive value for a robust optimization formulation, as shown in Figure 5. The arrival time of EVs is taken as 7am with an SOC of 0.2 and departure at 7pm with a target SOC of 0.8 for all the cases.

In order to visualize the impact of uncertainty of both buying and selling prices, three cases are simulated in this study. In the first case, uncertainty in only buying price is considered while in the second case, uncertainty in only selling price is considered. In the third case, uncertainty in both buying and selling prices are considered. Finally, operation costs are compared against different values of $\Gamma_{t,b}$ and $\Gamma_{t,s}$ for each case. The realization where $\Gamma_{t,b}$ and/or $\Gamma_{t,s}$ takes their respective maximum values is termed as a worst-case realization for that case.

B. UNCERTAINTY IN BUYING PRICE

In this section, four different cases are considered for evaluating the effect of uncertainty associated with the buying price. Nominal values of selling price are considered for all the cases in this section. In case a, nominal values of buying price are considered, i.e. $\Gamma_{t,b} = 0$. In case b, buying price uncertainty in the first 12 hours of the day is considered ($\Gamma_{t,b} = 0.5$, t $\in$ [1, 12]). In case c, buying price uncertainty in the last 12 hours of the day is considered ($\Gamma_{t,b} = 0.5$, t $\in$ [13, 24]). Finally, in case d, buying price uncertainty is considered in all time intervals of the day, i.e. $\Gamma_{t,b} = 1$. Case a is the nominal case and case d is the worst-case for this scenario.

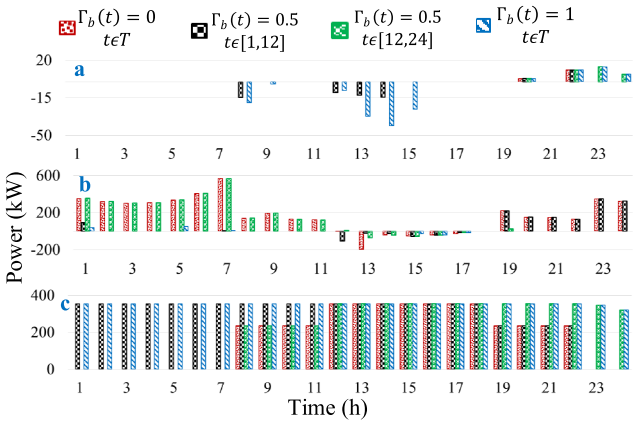

FIGURE 6. (a) Internal power transfer; (b) External power trading; (c) Power generation by CDGs.

It can be observed from Figure 6a that in nominal case, a small amount of internal power transfer is carried out in time intervals 20 and 22. In case b and case c, more power transfer can be observed due to the elevated buying prices in the respective uncertainty periods. In case d, internal power transfer is highest among all the cases due to uncertainty in all the time periods. In case b, external power trading and the generation amount of CDGs during time intervals 14-24 is identical to that of the nominal case as shown in Figure 6b and 6c. However, in the remaining 13 intervals due to increase in the buying price, generation of CDGs is increased to their fullest and buying from the utility grid is reduced. Similarly, in case c, external power trading and the generation amount of CDGs during time intervals 1-12 is identical to that of the nominal case. However, during time intervals 13-24, generation of CDGs is increased to their fullest and buying from the utility grid is reduced. Finally, in case d, generation of CDGs is increased to their fullest during the entire day. Buying from the utility grid is reduced and a small amount of power is bought when local CDGs cannot suffice the entire load demand.

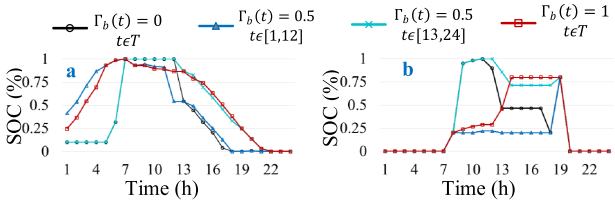

FIGURE 7. SOC of storage elements: (a) BESS units; (b) EVs.

It can be observed from Figure 7b that in all the cases, SOC of EVs is set to the target value (80%) before the departure time. The BESS charging pattern of case c is similar to that of the nominal case as shown in Figure 7a. In all the cases, BESS units are charged in the initial off-peak time intervals. BESS units are either used to avoid buying from the utility grid during the peak-price intervals or are used to sell power to the utility grid during higher price intervals to gain profit.

C. UNCERTAINTY IN SELLING PRICE

In this section, nominal values of market buying price along with uncertain selling price are considered. Similar to the previous section, case a is the nominal case, i.e. $\Gamma_{t,s} = 0$. In case b, uncertainty is considered in the first 12 hours of the operation horizon ($\Gamma_{t,s} = 0.5$, t $\in$ [1, 12]). In case c, uncertainty is considered in the last 12 hours of the operation horizon ($\Gamma_{t,s} = 0.5$, t $\in$ [13, 24]). In case d, selling price uncertainty is considered during the entire day, $\Gamma_{t,s} = 1$.

The amount of internal transfer in case b and case c is identical to that of the nominal case. However, in case d, due to reduced selling prices throughout the day, the internal transfer is increased, as shown in Figure 8a. In case a, CDGs are set to their maximum generation level and electricity is sold to the utility grid during higher selling price intervals to increase the profit. In case b, due to lower selling prices in the first 12 intervals, electricity is not sold to the utility grid during these intervals, as shown in Figure 8b. However, in the remaining intervals electricity is sold to the utility grid. In case c, generation to CDGs is reduced during time

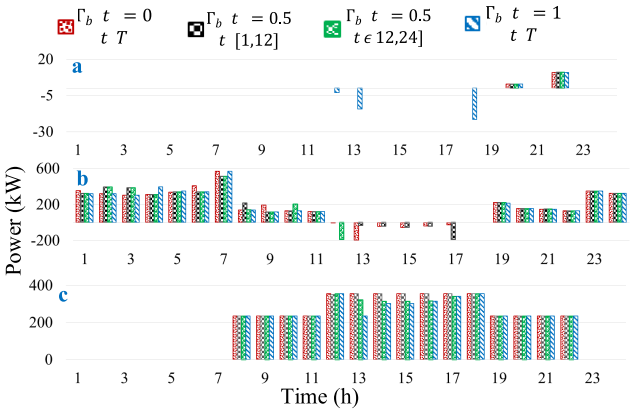

FIGURE 8. (a) Internal power transfer; (b) External power trading; (c) Power generation by CDGs.

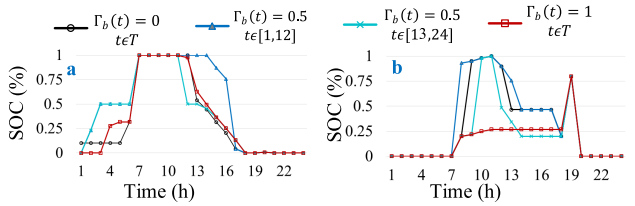

FIGURE 9. SOC of storage elements: (a) BESS units; (b) EVs.

intervals 13-17 to avoid selling, due to lower selling prices. In case d, due to lower selling prices throughout the day, selling is reduced to zero, as shown in Figure 8b. Similar to case c, generation of CDGs is equalized to the local load demand during time intervals 13-17. Case a is the nominal case and case d is the worst case for this scenario.

In all the cases, BESS units are charged during the off-peak time intervals. BESS units are discharged in the peak price intervals to reduce operation cost of the microgrid. BESS units are discharged and electricity is either sold to the utility grid or is used to suffice the local loads. Similar to the previous case, SOC of EVs is set to the target value (80%) before the departure time.

D. UNCERTAINTY IN BOTH BUYING & SELLING PRICE

In this section, uncertainty in both buying and selling prices is considered and four cases are simulated. Case a is the nominal case ($\Gamma_{t,s} = \Gamma_{t,b} = 0$) and case d is the worst-case ($\Gamma_{t,s} = \Gamma_{t,b} = 1$). In case b, uncertainty in buying and selling prices is considered during the first 12 intervals, i.e. $\Gamma_{t,s} = \Gamma_{t,b} = 0.5$, t $\in$ [1, 12]. In case c, uncertainty in buying and selling prices is considered during the last 12 intervals, i.e. $\Gamma_{t,s} = \Gamma_{t,b} = 0.5$, t $\in$ [1, 12].

In nominal case, internal power transfer between AC and DC microgrids is very low due to their ability to trade with the utility grid for increasing the profit. In case b and case c, electricity transfer can be observed during more time intervals. In case d, electricity transfer takes places during 8 time intervals, which is highest in all the cases as shown

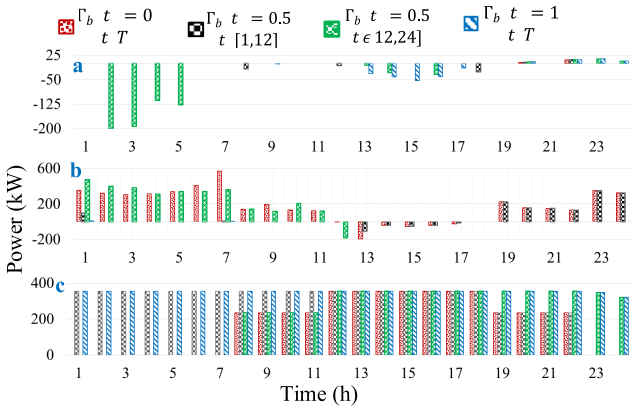

FIGURE 10. (a) Internal power transfer; (b) External power trading; (c) Power generation by CDGs.

in Figure 10a. In case b, the generation amount of CDGs is increased during first 12 intervals to avoid external trading as shown in Figure 10b and 10c. During these intervals, buying price has taken upper bounds and selling price has taken lower bounds. Therefore, trading with the utility grid during these intervals is not economical in case b. Similarly, in case c, generation of CDGs is increased during last 12 hours and external trading is reduced. Similar to case b, during the last 12 intervals trading with the utility grid is not economical in case c. Finally, in case d, generation of CDGs is increased during the entire day and trading with the utility grid is reduced. In case d, buying price has taken the upper uncertainty bound and selling price has taken the lower uncertainty bound during the entire day. Therefore, trading with the utility grid is not economical.

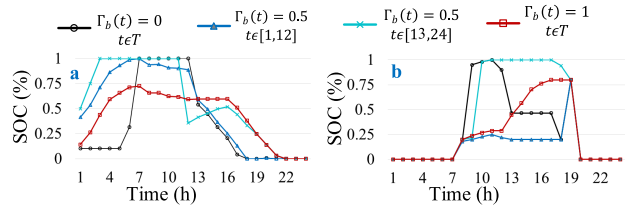

FIGURE 11. SOC of storage elements: (a) BESS units; (b) EVs.

Similar to the previous two cases, BESS units are charged during the off-peak intervals as shown in Figure 11a. BESS units are discharged and electricity is either sold to the utility grid or is used to fulfill the local load demand. It can be observed from Figure 11b that SOC of EVs is set to the specified target value (80%) before the departure time.

E. BUDGET OF UNCERTAINTY & OPERATION COST

The relationship between the budget of uncertainty for buying ($\Gamma_{t,b}$) and selling ($\Gamma_{t,s}$) prices and operation cost is tabulated in Table 3. Table 3 shows that the rise in operation cost in case of uncertainty in buying price is higher than that of the corresponding selling price. A limited amount of power has been sold to the utility grid in the nominal case; therefore,

TABLE 3. Relationship between budget of uncertainty & operation cost.

$\Gamma_{t,b}$	$\sum_{t\in T}\Gamma_{t,b}$	$\Gamma_{t,s}$	$\sum_{t\in T}\Gamma_{t,s}$	Cost (M₩)	Increase (%)
0	0	0	0	0.8845	0.0000
0.5[a]	12	0	0	0.9030	0.0210
0.5[b]	12	0	0	0.8906	0.0068
1	24	0	0	0.9092	0.0272
0	0	0.5[a]	12	0.8845	$3.05\text{x}10^{-5}$
0	0	0.5[b]	12	0.8861	0.0017
0	0	1	24	0.8873	0.0031
0.5[a]	12	0.5[a]	12	0.9031	0.0211
0.5[b]	12	0.5[b]	12	0.8917	0.0081
1	24	1	24	0.9093	0.0273
0	0	0	0	0.8845	0.0000
0.5[a]	12	0	0	0.9030	0.0210

[1]₩ is Korean Won (KRW), [a] indicates uncertainty in first 12 hours, and [b] indicates uncertainty in last 12 hours.

the effect of uncertainty in selling price is not prominent. Finally, the rise in operation cost is highest when both buying and selling prices are uncertain due to the avoidance of trading with the utility grid. The operation cost of the simulated hybrid microgrid will remain within the bounds of operation cost created by the nominal case ($\Gamma_{t,b} = \Gamma_{t,s} = 0$) and the worst-case ($\Gamma_{t,b} = \Gamma_{t,s} = 1$) scenarios, i.e. between 0.8845 million KRW and 0.9093 million KRW. This condition is valid, if the uncertainty bounds for buying and selling prices remain same. Other than nominal and worst-case scenarios (first and last row of Table 3), 8 other scenarios have been considered and simulated in this study. Table 3 shows that the operation costs of all the other 8 scenarios (2nd to the 9th row of Table 3) are within the upper and lower operation cost bound created by nominal and worst case scenarios.

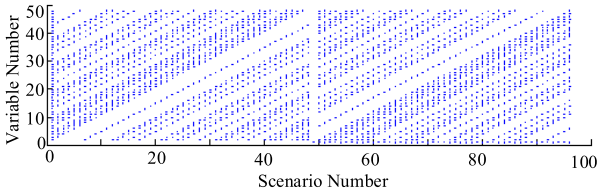

FIGURE 12. Taguchi's OA(96, 48, 2, 3) entries.

VI. ROBUSTNESS EVALUATION

The number of scenarios could be significantly high depending on the number of uncertain variables and their corresponding levels. It is not possible to test all the possible scenarios. In the simulated case, there are 24 uncertain variables for buying price and 24 for selling price. Therefore, there are total 48 uncertain variables in this study and two levels (0 and 1) are defined for each level. There would be a total of 2^{48} ways to generate uncertain variables, which is computationally expensive. Therefore, OA (96, 48, 2, 3) has been selected to test only limited scenarios. The OA has been taken from the online library [34] and each cycle contains only 96 scenarios, as shown in Figure 12. In Figure 12, dots represent a 1 and empty spaces represent a 0. Four different cycles are used to find the worst-case scenario from the selected OA. In cycle 1, buying price takes upper bounds and selling price takes lower bound if the value of the corresponding entity is 1 and take nominal values for 0. In cycle 2, 1 corresponds to upper bound for buying price and 0 corresponds to lower bound for selling price. In cycle 3, 1 corresponds to lower bound for selling price and 0 corresponds to upper bound for buying price. Finally, in cycle 4 buying price takes upper bounds and selling price takes lower bound if the value of the corresponding entity is 0 and take nominal values for 1. The operation cost for all the 96 scenarios in each cycle is shown in Figure 13. It can be observed from Figure 13 that the worst-case scenario occurred for cycle 2 and cycle 3 with an identical operation cost of 904212.2KRW, as highlighted.

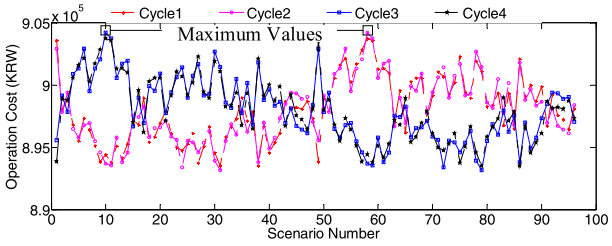

FIGURE 13. Operation cost of Taguchi's under different cycles.

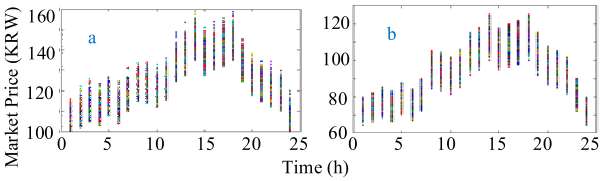

FIGURE 14. Ten thousand Monte Carlo scenarios: (a) Buying price; (b) Selling price.

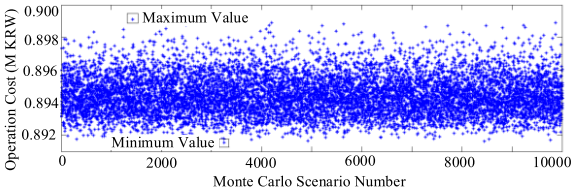

FIGURE 15. Operation cost of 10 Thousand Monte Carlo scenarios.

Monte Carlo simulations are used to generate 10000 scenarios for both buying and selling price signals. As mentioned in Section 4.1, the region between nominal values and upper bounds is used for buying price scenario generation. Similarly, the region between nominal values and lower bounds is used for generating selling price signal scenarios. The Monte Carlo-based scenarios for buying and selling prices are shown in Figure 14. The operation cost for all the ten thousand scenarios is shown in Figure 15. It can be observed from Figure 15 that the maximum value of the operation cost is for scenario number 1423, which is 899123.1KRW. The value of daily operation cost obtained in the worst-case

scenario of OA would remain biggest in most of the scenarios produced within the uncertainty bounds of buying and selling prices. The maximum value among all the scenarios is lesser than that of the OA's worst-case scenario, i.e. $\nu = 0$. This indicates that the selected testing scenario based on OA is representative and works well for robust worst-case selection in the uncertain environment. On the other hand, the minimum value of operation cost occurred at scenario number 3250, which is 891552.1KRW. Even this minimum value is also greater than the operation cost of the nominal case, which is 884485.6KRW. The value of ν for the forecasted case is 100%, i.e. no robustness. The average cost deviation of all the scenarios from the selected worst-case scenarios comes out to be 4659.2KRW, which was 9978.2KRW for the deterministic case. This shows the reduction of fluctuations in operation cost by 53.31% for the proposed robust method.

VII. CONCLUSION

In order to access the effect of market price uncertainties on the operation of hybrid microgrids, a robust optimization method is utilized for optimal operation of hybrid microgrids. In contrast to the existing literature, where stochastic scenario-based optimization techniques are used for the realization of market price uncertainties, a worst-case scenario based optimization technique is utilized in this paper. Accurate information regarding the probability density of the uncertain parameter is not required and only a deterministic set of bounds are required. In addition, the computational complexity and tractability of the problem are assured, even for large systems. The developed mixed integer linear programming-based model can assure immunity against the worst-case scenario if the uncertainty is within the specified bounds. The determined unit commitment status of CDGs and BESS units remains valid even if the buying and/or selling prices fluctuate within the determined bounds of uncertainties. There is an inverse relationship between the operation cost and the probability of infeasible solution. Therefore, a trade-off needs to be decided by the decision makers by selecting an appropriate value for the budget of uncertainty variable. Simulation results show that the effect of uncertainty in buying price on operation cost of the microgrid is more prominent as compared to the corresponding selling price uncertainty. The rise in operation cost is highest when both buying and selling prices are uncertain. The worst-case scenario selected by the Taguchi's OA method and its robustness has been demonstrated by the Monte Carlo simulations. The average cost fluctuations are reduced by 53.31% by the proposed method.

REFERENCES

[1] K. Boroojeni, M. H. Amini, A. Nejadpak, T. Dragičević, S. S. Iyengar, and F. Blaabjerg, "A novel cloud-based platform for implementation of oblivious power routing for clusters of microgrids," *IEEE Access*, vol. 5, pp. 607–619 Dec. 2016.

[2] F. Farzan, S. A. Vaghefi, K. Mahani, M. A. Jafari, and J. Gong, "Operational planning for multi-building portfolio in an uncertain energy market," *Energy Build.*, vol. 103, pp. 271–283, Sep. 2015.

[3] M. Ortiz, O. Ukar, F. Azevedo, and A. Múgica, "Price forecasting and validation in the Spanish electricity market using forecasts as input data," *Int. J. Elect. Power Energy Syst.*, vol. 77, pp. 123–127, May 2016.

[4] E. E. Elattar, "Day-ahead price forecasting of electricity markets based on local informative vector machine," *IET Generat., Transmiss., Distrib.*, vol. 7, no. 10, pp. 1063–1071, Oct. 2013.

[5] G. Aneiros, J. Vilar, and P. Raña, "Short-term forecast of daily curves of electricity demand and price," *Int. J. Elect. Power Energy Syst.*, vol. 80, pp. 96–108, Sep. 2016.

[6] H. Zareipour, C. A. Canizares, and K. Bhattacharya, "Economic impact of electricity market price forecasting errors: A demand-side analysis," *IEEE Trans. Power Syst.*, vol. 25, no. 1, pp. 254–262, Feb. 2010.

[7] P. Mathuria and R. Bhakar, "GenCo's integrated trading decision making to manage multimarket uncertainties," *IEEE Trans. Power Syst.*, vol. 30, no. 3, pp. 1465–1474, May 2015.

[8] A. Soroudi, P. Siano, and A. Keane, "Optimal DR and ESS scheduling for distribution losses payments minimization under electricity price uncertainty," *IEEE Trans. Smart Grid*, vol. 7, no. 1, pp. 261–272, Jan. 2016.

[9] J. S. Shen, C. W. Jiang, Y. Y. Liu, and X. Wang, "A microgrid energy management system and risk management under an electricity market environment," *IEEE Access*, vol. 4, pp. 2349–2356, Apr. 2016.

[10] A. Gholami, T. Shekari, F. Aminifar, and M. Shahidehpour, "Microgrid scheduling with uncertainty: The quest for resilience," *IEEE Trans. Smart Grid*, vol. 7, no. 6, pp. 2849–2858, Nov. 2016.

[11] S. Nojavan, B. Mohammadi-Ivatloo, and K. Zare, "Optimal bidding strategy of electricity retailers using robust optimisation approach considering time-of-use rate demand response programs under market price uncertainties," *IET Generat., Transmiss., Distrib.*, vol. 9, no. 4, pp. 328–338, Mar. 2015.

[12] G. Liu, Y. Xu, and K. Tomsovic, "Bidding strategy for microgrid in day-ahead market based on hybrid stochastic/robust optimization," *IEEE Trans. Smart Grid*, vol. 7, no. 1, pp. 227–237, Jan. 2016.

[13] Y. Zhang, N. Gatsis, and G. B. Giannakis, "Robust energy management for microgrids with high-penetration renewables," *IEEE Trans. Sustainable Energy*, vol. 4, no. 4, pp. 944–953, Oct. 2013.

[14] J. M. Lujano-Rojas, G. J. Osório, and J. P. S. Catalão, "New probabilistic method for solving economic dispatch and unit commitment problems incorporating uncertainty due to renewable energy integration," *Int. J. Elect. Power Energy Syst.*, vol. 78, pp. 61–71, Jun. 2016.

[15] A. Hussain, V. H. Bui, H. M. Kim, Y. H. Im, and J. Y. Lee, "Optimal operation of tri-generation microgrids considering demand uncertainties," *Int. J. Smart Home*, vol. 10, no. 10, pp. 131–144, Oct. 2016.

[16] L. Jian, H. Xue, G. Xu, X. Zhu, D. Zhao, and Z. Y. Shao, "Regulated charging of plug-in hybrid electric vehicles for minimizing load variance in household smart microgrid," *IEEE Trans. Ind. Electron.*, vol. 60, no. 8, pp. 3218–3226, Aug. 2013.

[17] A. Hussain, V. H. Bui, and H. M. Kim, "Robust optimization-based scheduling of multi-microgrids considering uncertainties," *Energies*, vol. 9, no. 4, pp. 278–298, Apr. 2016.

[18] Y. Xiang, J. Liu, and Y. Liu, "Robust energy management of microgrid with uncertain renewable generation and load," *IEEE Trans. Smart Grid*, vol. 7, no. 2, pp. 1034–1043, Mar. 2016.

[19] H. Han, S. Gao, Q. Shi, H. Cui, and F. Li, "Security-based active demand response strategy considering uncertainties in power systems," *IEEE Access*, vol. 5, pp. 16953–16962, Aug. 2017.

[20] S. Pazouki and M.-R. Haghifam, "Optimal planning and scheduling of energy hub in presence of wind, storage and demand response under uncertainty," *Int. J. Elect. Power Energy Syst.*, vol. 80, pp. 219–239, Sep. 2016.

[21] A. Soroudi, "Possibilistic-scenario model for DG impact assessment on distribution networks in an uncertain environment," *IEEE Trans. Power Syst.*, vol. 27, no. 3, pp. 1283–1293, Aug. 2012.

[22] D. Bertsimas and M. Sim, "The price of robustness," *Oper. Res.*, vol. 52, no. 1, pp. 35–53, Feb. 2014.

[23] A. Hussain, V. H. Bui, and H. M. Kim, "Optimal operation of hybrid microgrids for enhancing resiliency considering feasible islanding and survivability," *IET Renew. Power Generat.*, vol. 11, no. 6, pp. 846–857, May 2017.

[24] A. Soroudi, "Taxonomy of uncertainty modeling techniques in renewable energy system studies," *Large Scale Renewable Power Generation*. Singapore: Springer, 2014.

[25] M. S. Mahmoud, M. Saif Ur Rahman, and F. M. A. L. Sunni, "Review of microgrid architectures—A system of systems perspective," *IET Renew. Power Generat.*, vol. 9, no. 8, pp. 1064–1078, Nov. 2015.

[26] D. Kumar, F. Zare, and A. Ghosh, "DC microgrid technology: System architectures, AC grid interfaces, grounding schemes, power quality, communication networks, applications, and standardizations aspects," *IEEE Access*, vol. 5, pp. 12230–12256, Jun. 2017.
[27] D. Bertsimas and M. Sim, "Robust discrete optimization and network flows," *Math. Programm.*, vol. 98, no. 1, pp. 49–71, 2003.
[28] A. Bidram and A. Davoudi, "Hierarchical structure of microgrids control system," *IEEE Trans. Smart Grid*, vol. 3, no. 4, pp. 1963–1976, Dec. 2012.
[29] T. Dragicevic, J. M. Guerrero, J. C. Vasquez, and D. Skrlec, "Supervisory control of an adaptive-droop regulated DC microgrid with battery management capability," *IEEE Trans. Power Electron.*, vol. 29, no. 2, pp. 695–706, Feb. 2014.
[30] A. Khosravi, S. Nahavandi, D. Creighton, and A. F. Atiya, "Lower upper bound estimation method for construction of neural network-based prediction intervals," *IEEE Trans. Neural Netw.*, vol. 22, no. 3, pp. 337–346, Mar. 2011.
[31] A. Khosravi, S. Nahavandi, and D. Creighton, "Construction of optimal prediction intervals for load forecasting problems," *IEEE Trans. Power Syst.*, vol. 25, no. 3, pp. 1496–1503, Aug. 2010.
[32] A. S. Hedayat, N. J. A. Sloane, and J. Stufken, *Orthogonal Arrays: Theory and Applications*. New York, NY, USA: Springer, 1999.
[33] Y. Wu, and A. Wu, *Taguchi Methods for Robust Design*. New York, NY, USA: ASME, 2000.
[34] N. J. A. Sloane. *A Library of Orthogonal Arrays*. Accessed: Jan. 24, 2018. [Online]. Available: http://neilsloane.com/oadir
[35] A. Barvinok, *A Course in Convexity*, vol. 54. Providence, RI, USA: AMS, 2002.
[36] G. Hongjun, J. Liu, Z. Wei, Y. Cao, W. Wang, and S. Huang, "A security-constrainted dispatching model for wind generation units based on extreme scenario set optimization," *Power Syst. Technol.*, vol. 37, no. 6, pp. 1590–1595, May 2013.

AKHTAR HUSSAIN (S'14) received the B.E. degree in telecommunications from the National University of Sciences and Technology, Pakistan, in 2011, and the M.S. degree in electrical engineering from Myongji University, Yongin, South Korea, in 2014. He is currently pursuing the Ph.D. degree with Incheon National University, South Korea. From 2014 to 2015, he was an Associate Engineer at IEDs development company, SANION, South Korea. His research interests are power system automation and protection, smart grids, and microgrid optimization.

VAN-HAI BUI (S'16) received B.S. degree in electrical engineering from the Hanoi University of Science and Technology, Vietnam, in 2013. He is currently pursuing the combined master's and Ph.D. degrees with the Department of Electrical Engineering, Incheon National University, South Korea. His research interests include microgrid operation and energy management system.

HAK-MAN KIM (SM'15) received the Ph.D. degree in electrical engineering from Sungkyunkwan University, South Korea, in 1998, and the second Ph.D. degree in information sciences from Tohoku University, Japan, in 2011, respectively. He was with the Korea Electrotechnology Research Institute, South Korea, from 1996 to 2008. He is currently a Professor with the Department of Electrical Engineering, Incheon National University, South Korea. His research interests include microgrid operation and control, and dc power systems.